Skeletal Radiol (2011) 40:1261–1273
DOI 10.1007/s00256-010-0971-8

REVIEW ARTICLE

Imaging pattern of calvarial lesions in adults

Jarred Garfinkle · Denis Melançon · Maria Cortes · Donatella Tampieri

Received: 30 January 2010 / Revised: 5 May 2010 / Accepted: 11 May 2010 / Published online: 6 June 2010

Abstract Calvarial lesions often present themselves as clinically silent findings on skull radiographs or as palpable masses that may cause localized pain or soreness. This review aims to explore the radiographic, computed tomography (CT), and magnetic resonance imaging (MRI) characteristics of calvarial neoplastic, inflammatory, and congenital lesions that are common in adults in order to facilitate a structured approach to their diagnosis and limit the differential diagnosis. In addition to reviewing the literature, we reviewed the records of 141 patients of the Montreal Neurological Institute and Hospital with radiologically documented calvarial lesions between 2001 and June 2009. CT is ideal for detecting bony lesions and is helpful in precisely localizing a lesion pre-surgically. MRI is best at identifying intradiploic lesions before they affect the cortical tables and is able to establish extraosseous involvement, especially when paramagnetic contrast is employed.

Keywords Calvaria · Neoplasm · Lesion · MRI · CT

Calvarial lesions often present themselves as clinically silent findings on skull radiographs or as palpable masses that may cause localized pain or soreness. Since a variety of neoplastic, inflammatory, congenital, and traumatic etiologies can give rise to such lesions, an organized approach to their diagnosis is essential. To achieve an accurate diagnosis is important because although most calvarial lesions are benign, those that are malignant require adequate therapy [1].

Radiography is often the first imaging modality used to evaluate a calvarial lesion and can often suggest a diagnosis [2]. Computed tomography (CT) and/or magnetic resonance imaging (MRI) commonly follow. CT is ideal for detecting bone lysis and sclerosis, determining the involvement of each of the two skull tables and the diploë, and is helpful in precisely localizing and delineating a lesion pre-surgically. CT can also demonstrate calcification within a lesion and the presence of sclerotic margins. MRI is able to show intradiploic lesions before they erode the cortical tables; moreover, if the radiographs suggest soft tissue or intraaxial involvement, then MRI is preferable due to its ability to establish extraosseous involvement, especially when paramagnetic contrast is employed [3].

This review explores the radiographic, CT, and MRI imaging characteristics of neoplastic, inflammatory, and congenital lesions that are common in adults (18 years and older) in order to facilitate a structured approach to their diagnosis.

For this review, we reviewed the images of all the patients of the Montreal Neurological Institute and Hospital (MNI) with radiologically documented calvarial lesions between 2001 and June 2009. We reviewed 141 lesions that either directly affected or secondarily affected the calvaria. Of these, 54 lesions (38%) had surgical or pathologic correlation and are herein used to illustrate the imaging qualities of the various lesions. The most common lesions encountered were: 32 osteomas (23%); 22 eosinophilic granulomas or Langerhans cell histiocytoses (16%); 18 hemangiomas and meningiomas each (13% each); 14 fibrous dysplasias and metastases each (10% each); six squamous or basal cell carcinomas (4%); five multiple myelomas (4%); and 12 other lesions (9%). Other lesions include: epidermoid cyst (four), lipoma (two), dermoid cyst (one), ossifying fibroma (one), hemangiopericytoma

J. Garfinkle (✉) · D. Melançon · M. Cortes · D. Tampieri
Department of Diagnostic and Interventional Neuroradiology,
Montreal Neurological Institute and Hospital-McGill
University Health Center,
3801 Rue University,
Montreal, Quebec, Canada
e-mail: jarred.garfinkle@mail.mcgill.ca

(one), lymphoma (one), and aneurysmal bone cyst (one). Eleven cases of Paget's disease, none of which featured sarcomatous transformation, were also encountered. Meningiomas, hemangiopericytomas, and squamous or basal cell carcinomas typically invade the calvaria secondarily, whereas all of the other aforementioned lesions originate from within the calvaria.

Radiological approach to the evaluation of calvarial lesions

Anatomy and imaging

The calvaria comprise the frontal bone, parietal bones, occipital bone, squamous and zygomatic portions of the temporal bones, and the tips of the greater wings of the sphenoid bones [4]. In terms of layers, the inner and outer tables of cortical bone sandwich the diploë, which contains cancellous bone and bone marrow. Some lesions may extend beyond these three layers into the scalp or the meninges. Other lesions originate in the scalp or meninges and invade the adjacent bone. Some calvarial lesions have a partiality towards particular bones, and many have a tendency to involve extraosseous components.

On CT, the calvaria is best evaluated using a bone algorithm or at least when viewed using bone windows. On MRI, the cortical tables appear as signal void on both T1-weighted images (T1WI) and T2-weighted images (T2WI). In adults, the marrow has high signal intensity on T1WI due to the high fat content. In adolescents, the marrow signal is more heterogeneous because the marrow is not yet completely replaced with fat; nonetheless, the signal tends to be bilaterally symmetrical [4]. Except for diploic veins and meninges adjacent to Pacchionian granulations, the diploë does not normally enhance with contrast [5].

Certain imaging signs indicate that a lesion is extraaxial (i.e., lies outside the brain parenchyma). Typically, extraaxial masses cause local bony changes [6]. The next most reliable sign is the displacement of pial arteries or veins away from the bone or dura. White matter buckling, which describes the process whereby the white matter is compressed while the edema-resistant grey matter is spared, is unique to extraaxial lesions [7]. Furthermore, on MRI, a CSF cleft, which is hypointense on T1WI and hyperintense on T2WI, can be found between the lesion and the brain.

Borders of the lesion and types of bone destruction

A lesion's borders and its type of bone destruction are indicative of its growth rate and consequently its benignity or malignancy. A clearly demarcated lesion with a narrow zone of transition and a uniform area of destruction suggests slow growth, whereas an ill-defined margin with a wide zone of transition and permeative destruction suggests a more aggressive lesion [8]. The development of a sclerotic margin suggests a long-standing lesion with "remodeling" behavior while the absence of a sclerotic border is more consistent with an aggressive process.

Periosteal response

The outer table is covered by periosteum and the periosteum of the inner table is included in the dura. Calvarial lesions are not typically associated with a periosteal reaction because the periosteum cannot be identified on CT or MRI [4].

Soft tissue and dural extension

The cortical tables may contain slow-growing lesions; however, aggressive lesions may extend through destroyed bone into soft tissue, dura mater, and/or brain parenchyma [8]. On MRI, the dura mater adjacent to malignant lesions is often thickened and often enhances after contrast administration, reflecting the lesion's tendency to invade or inflame it [9, 10]. Dural enhancement can also reflect a benign lesion or even normal meninges [11]. Nodular, discontinuous enhancement is associated with invasion, whereas continuous, linear enhancement is typically an expression of a reactive change. A thin hypointense line between the lesion and the enhanced dura implies the persistence of the potential epidural space, which itself suggests that the dura mater remains uninvaded [12].

Calvarial lesions

Eosinophilic granuloma

Langerhans cell histiocytosis (LCH) encompasses three idiopathic diseases that are characterized by proliferation of Langerhans cells [13]. When it is solitary and monostotic, as is most often the case, the lesion is referred to as an eosinophilic granuloma. LCH occurs most commonly in children and adolescents and its severity is inversely related to the age of onset. The lesion's quick progression and rapid regression are salient features. The calvaria is the most common site for LCH, with the parietal bones most frequently affected.

The lesion is usually lytic with well-defined non-sclerotic borders and involves all three layers of the skull (Fig. 1). A sclerotic margin may appear if the lesion begins

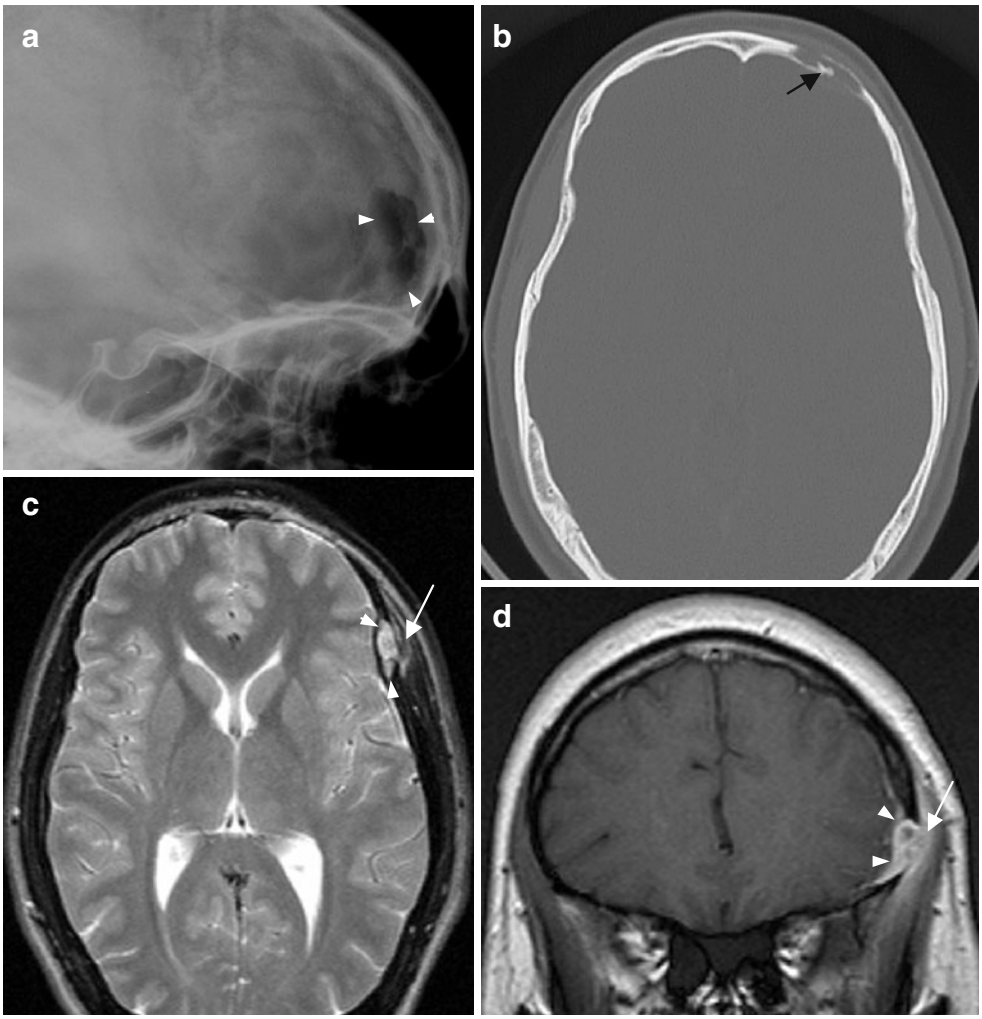

Fig. 1 Multifocal LCH of the skull in a 21-year-old man. **a** Lateral skull radiograph of the patient pre-surgery showing a well-defined osteolytic lesion in the frontal bone with a double contour *(arrowheads)*. **b** Bone algorithm of an infused CT showing the borders of the lesion and a button sequestrum *(arrow)* within it. **c** MRI taken 5 months later, post-surgically, showing the area of excision and a new lesion at the left fronto-temporal junction. On axial T2WI, the lesion demonstrates heterogeneously higher signal than grey matter while on coronal-enhanced T1WI (**d**) showing marked enhancement *(arrowheads)*. Note that in both MR images, the lesion appears to have extended into the temporal fossa and involves the temporal muscle *(arrow)*

to regress, as normal bone replaces the inflammatory cell infiltrate [14]. The beveled edge or double-contoured appearance of the lesion, which is caused by uneven destruction of the two cortical tables, is highly suggestive of LCH on skull radiographs [4]. The granulomas are slightly denser than grey matter on CT [15]. Residual bone, referred to as a "button sequestrum," may be present in the osteolytic lesion but is a relatively uncommon finding in our experience. On MRI, the lesion appears hypo-isointense to grey matter on T1WI and heterogeneously hyperintense on T2WI. It enhances markedly. The adjacent dura usually enhances as well, but is rarely penetrated [16, 17]. As opposed to eosinophilic granuloma of the appendicular skeleton, that of the calvaria does not appear to be associated with edema of the surrounding marrow and soft tissue, as none of the nine eosinophilic granulomas imaged with MRI herein reviewed featured surrounding edema. In our experience, when the diagnosis of eosinophilic granuloma is suspected but tentative, a follow-up CT is helpful in affirming the diagnosis because spontaneous resolution is common.

Epidermoid and dermoid

Both epidermoids and dermoids are congenital unilocular ectodermal inclusion cysts lined by an epithelium. Epidermoid cysts are filled with debris (keratin and cholesterol) from the desquamation of their thin squamous epithelial lining whereas dermoid cysts are lined by a thicker epithelium and filled with sebaceous, sweat and apocrine glands, hair, and less commonly, teeth. Epidermoids tend to present more laterally and during the third and fourth decades of life while dermoids usually present closer to the midline or around the orbit and during the second and third decades of life [18].

Radiographically, intradiploic epidermoid and dermoid cysts erode and may expand both the inner and outer tables of the calvaria and typically feature a smooth sclerotic rim pursuant to bone remodeling (Fig. 2). On CT, epidermoids are homogeneous and are similar in density to cerebrospinal fluid. Dermoids differ in that they are more heterogeneous and may display calcification along their wall or internally [19, 20]. On MRI, epidermoids are invariably hyperintense on T2WI and of variable intensity on T1WI. In contrast,

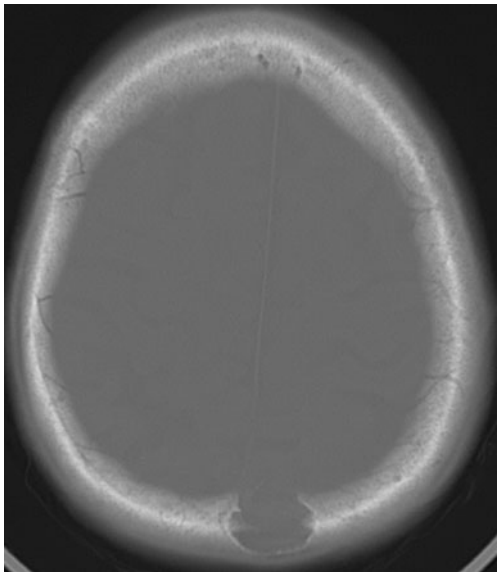

Fig. 2 Epidermoid cyst in a 78-year-old woman. CT with bone algorithm shows a fully lucent lesion with a sclerotic margin in the occipital bone

most dermoids have the signal intensity characteristics of fat on MRI due to their oily sebaceous secretions (Fig. 3). As such, they are often hyperintense on both T1 and T2WI. Neither the wall nor the interior of the epidermoid enhance upon contrast administration on CT or MRI. The wall of the dermoid, however, may enhance, as it is often somewhat vascularized [21].

Hemangioma

Hemangiomas are benign blood vessel tumors with a higher predilection for women in the middle decades of life [22]. They are most often seen solitarily in the frontal and parietal bones but can affect any region of the calvaria. Most calvarial hemangiomas are histologically classified as cavernous, meaning that they are composed of dilated blood vessels contained within the bony trabeculae.

The calvarial hemangioma is radiographically characterized by a lytic lesion with a "sunburst" or "honeycomb" trabecular matrix radiating from a common center (Fig. 4). The trabecular pattern, which is not invariably present, may be the result of osteoclastic activity pursuant to the stress caused by vascular neoplasia and the ensuing osteoblastic remodeling [23]. Originating intradiploically, the lesion usually expands the outer table, thus often eroding it and leaving the inner table intact. As it grows further, the inner table can be displaced as well, and may also become eroded. It is usually sharply separated from normal bone and a reactive sclerosis is present in approximately 30% of cases. MRI T1WI shows a mottled isointense lesion within the diploic space with scattered hypo-and hyperintensities corresponding to iron storage complexes and fatty tissue, respectively. T2WI reveals a hyperintense lesion, indicating the presence of the aforementioned iron storage complexes [24]. A larger lesion may show more hypointense foci secondary to thickened trabeculae. During rapid serial MRI, hemangiomas show a characteristic imaging enhancement pattern in that they enhance in focal areas during the early phase and enhance diffusely during the later phase. The adjacent meninges may also enhance [25]. In our experience, smaller hemangiomas may be more difficult to distinguish from eosinophilic granulomas, probably because the lesion's sunburst matrix seems to be less apparent when the lesion is relatively small.

Meningioma

Meningioma represents the most common benign intracranial neoplasm. This tumor arises from the meningothelial cells and usually forms a unilobular mass with a broad-based dural attachment [26]. Meningiomas are less commonly malignant. The parasagittal region is a common site. It may cause surrounding edema by pressuring the subjacent parenchyma. Bony changes occur in approxi-

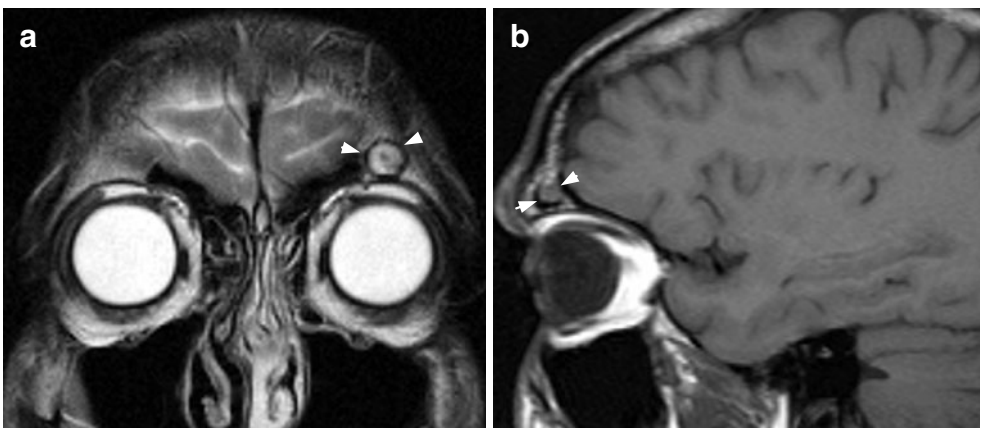

Fig. 3 Dermoid cyst in a 32-year-old man. **a** Coronal T2WI demonstrating the well-circumscribed, predominantly hyperintense mass in the left superior orbital roof *(arrowheads)*. **b** Axial T1WI depicting the well-defined lesion with a signal intensity similar to that of grey matter, suggesting a low fat content *(arrowheads)*. The thin hypointense line surrounding the lesion represents a dense sclerotic margin

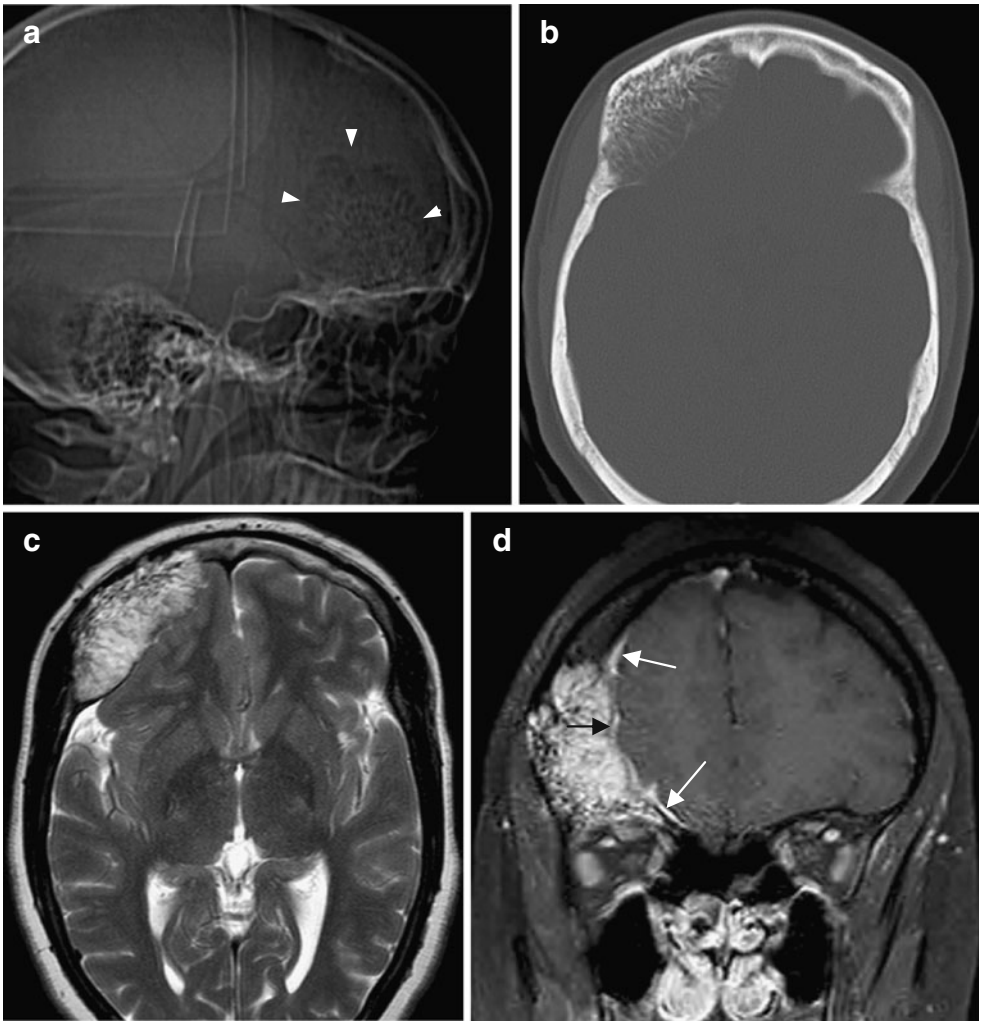

Fig. 4 Hemangioma in a 30-year-old woman who presented with worsening headaches, blurred vision, and right proptosis. **a** Scout CT showing the radiating "honeycomb" trabecular pattern of this frontal well-circumscribed lesion *(arrowheads)*. **b** CT with bone algorithm showing an expanded lesion that erodes the inner table more than the outer table and contains radiating trabeculae with mass effect on the adjacent frontal lobe. **c** T2WI showing a hyperintense mass. **d** Contrast-enhanced coronal T1WI also showing enhancement of the mass and a dural tail sign *(white arrows)*. The *thin hypointense line* denotes the epidural space, thus suggesting that the dural enhancement is reactive rather than infiltrative *(black arrow)*. Note that the lesion reveals heterogeneous intensities in all MRI images due to the bony trabeculae

mately one-quarter of meningiomas [27]. Hyperostosis (bone formation) is the most common bony change, but bone destruction sometimes also occurs. Plaque meningiomas coat the inner table and are more likely to cause hyperostosis than the more pedunculated globular sort. These plaque meningiomas are relatively prone to infiltrating the underlying dura and overlying bone. About 1% of meningiomas originate ectopically within the diploë. These are commonly referred to as intraosseous meningiomas [28].

CT typically shows a round or smoothly lobulated mass that appears hyperdense to brain parenchyma in 75% of cases and isodense in the rest (Fig. 5). Focal, diffuse, rim-like or punctate calcification is seen in 20% of cases [27]. Contrast-enhanced CT generally shows intense, uniform enhancement, but 10–15% of cases show an atypical pattern [29]. On T1WI, it is usually hypo-isointense, while on T2WI it is usually iso-hyperintense, and sometimes heterogeneous. It enhances homogeneously and often exhibits a dural tail. Enhanced MR images are particularly able to detect small meningiomas that appear isointense on other MR images. The dural tail sign, which describes peritumoral-enhanced dura, is suggestive of, but not specific to, meningiomas [9]. Intraosseous meningiomas usually extend through the cortical tables into the adjacent soft tissues. The intraosseous meningioma can be radiologically indistinguishable from the plaque variety if by the time of presentation, the intraosseous meningioma has already infiltrated the dura. In these cases, the true origins of the tumor cannot be stated with certainty [30]. Nonetheless, prominent hyperostosis and minimal intracranial presence are more suggestive of the intraosseous sort while associated edema is more suggestive of the plaque variety.

Hemangiopericytoma

Hemangiopericytomas, which can arise from pericytes around the meninges, are low-grade malignant tumors that typically present in young people [31]. The pericytes around the meninges are particularly prone to neoplastic changes and as such, calvarial hemangiopericytomas are often misdiagnosed as malignant meningiomas. Moreover, they have a predilection for the same sites as meningiomas,

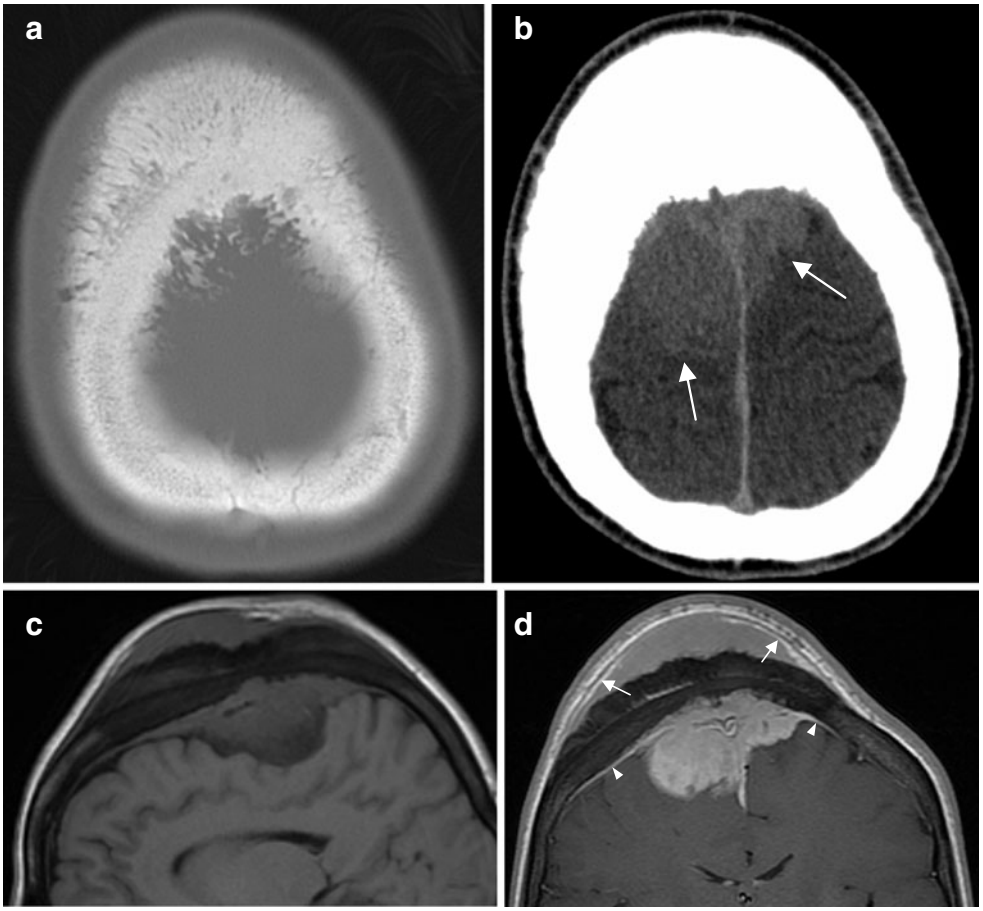

Fig. 5 Typical plaque meningioma of the vertex in a 43-year-old woman. **a** Bone algorithm CT clearly demonstrating hyperostosis and tumor transgression across the bone in the form of spiculation while on soft tissue CT (**b**), the tumor appears isodense to the cortex *(arrows)*. **c** Sagittal T1WI confirms the CT findings (particularly the hyperostosis of the outer table) and shows the isointense lesion extending subgalealy. **d** Contrast-enhanced coronal T1WI showing an avidly enhancing lesion occluding the superior sagittal sinus. Note the dural tail sign *(arrowheads)* and the reactive galeal enhancement *(arrows)*

such as the parasagittal region. Hemangiopericytomas have a particular tendency towards delayed extraneural metastasis, with an average period of 99 months before metastasis. About three-quarters of them metastasize by 15 years post-resection [32]. The same biologic behavior can apply to those lesions mistakenly labeled as malignant meningiomas, which may be rediagnosed as hemangiopericytomas following a skeletal metastasis [33].

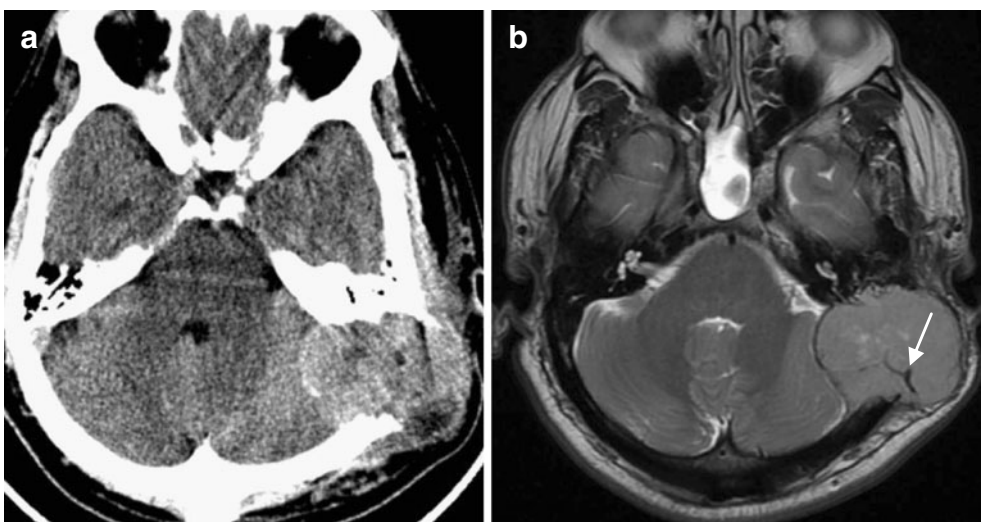

Fig. 6 Hemangiopericytoma in a 48-year-old woman originally diagnosed as a lytic intraosseous meningioma. **a** Axial CT scan showing an isodense mass with an incomplete sclerotic margin that has obliterated the adjacent bone. **b** Axial T2WI showing an extradural polylobulated mass that appears isointense and extends both intra-and extracranially. Note the signal void that represents a vascular channel within the lesion *(arrow)*

Meningeal hemangiopericytomas, in contrast to meningiomas, do not exhibit calcification, frequently cause bony erosion, and almost never cause hyperostosis (Fig. 6). Their irregular or lobulated borders and heterogeneous enhancement pattern reflect their aggressive nature. There is less often peritumoral edema in hemangiopericytomas. Furthermore, although meningiomas may have internal vascular signal voids, this finding is more common in hemangiopericytomas [34].

Fibrous dysplasia

Fibrous dysplasia is a genetically based sporadic disorder haracterized by the replacement of normal cancellous bone with abnormal fibrous tissue containing immature woven bone [8]. This benign lesion typically occurs in adolescents and young adults and may involve a single bone (monostotic) or multiple bones (polyostotic). Fibrous dysplasia of the calvaria usually affects the frontal or temporal bones [35].

The woven bone component of the lesion results in the characteristic radiographic "ground glass" appearance (Fig. 7). All cases described in the literature demonstrate some degree of this hazy, intradiploic density on CT, making CT the investigation of choice and the most useful diagnostic tool for fibrous dysplasia in our experience. The radiographic density corresponds to the degree of mineralization of the lesion. The lesion usually causes the outer table to bulge outward while conserving the shape of the inner table [17]. Moreover, it is usually bound by a prominent sclerotic margin [36]. It is hypointense on T1WI, but more fibrous areas tend to relatively isointense. The T2WI appearance is heterogeneous and variable, with more fibrous areas that include fewer bony trabeculae and less cellularity showing high signal and low signal indicating a more osseous and cellular matrix. A peripheral black ring representing the sclerotic border is typically seen on MRI. Contrast enhancement is also variable: it can be homogeneous, central, or affect only the periphery [37]. In this pathology, MRI is most valuable in delineating the full extent of the lesion.

Osteoma

Osteoma is a benign, painless, slow-growing tumor comprising mature bone. It represents the most frequent calvarial tumor, and in our series, was almost invariably discovered incidentally [4]. It most commonly grows from the outer table of the calvaria, but can also originate from the inner table.

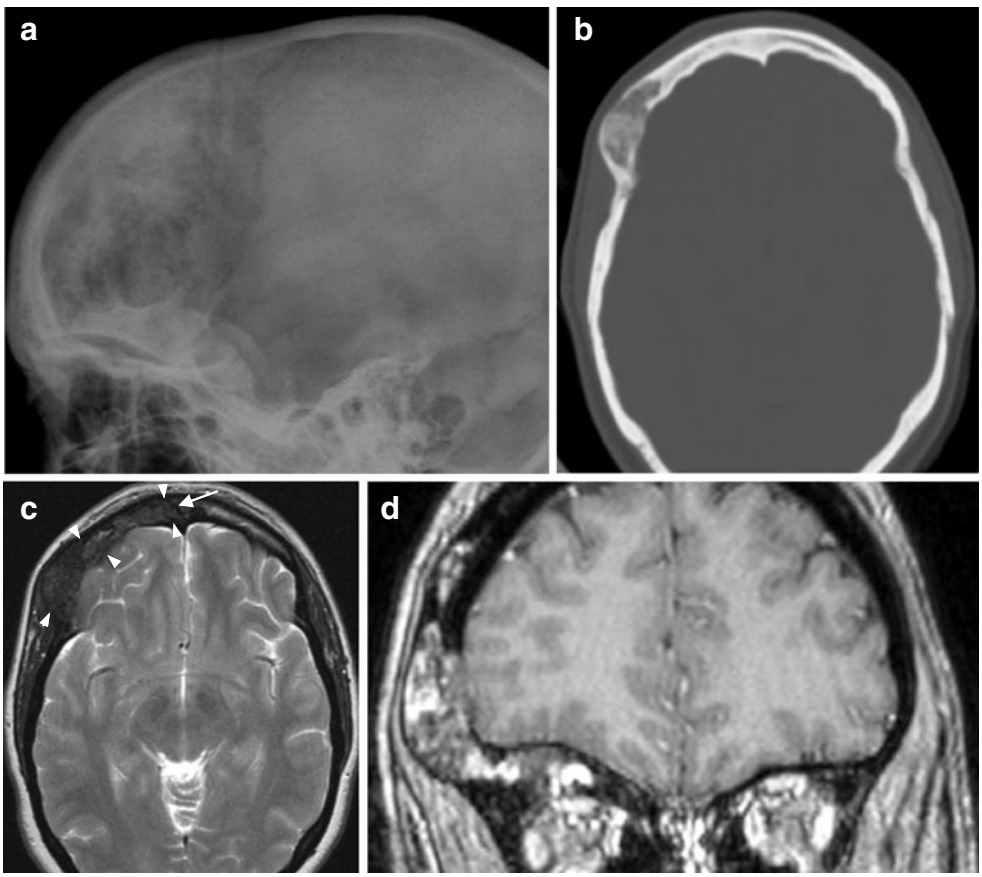

Fig. 7 Fibrous dysplasia in a 27-year-old woman. **a** Lateral radiograph demonstrating the typical ground-glass appearance of the well-demarcated lesion in the frontal region. **b** CT in bone window revealing an expanded, mottled diploë and thinning of both cortical tables in the right frontal bone. **c** Axial T2WI showing a heterogeneously hypointense expanded lesion that extends supraorbitally *(arrowheads)*. The *thin hypointense line* represents a dense sclerotic rim (*arrow*). **d** Reformatted coronal contrast-enhanced T1WI showing areas with and without contrast enhancement and clearly demonstrating the extent of the lesion

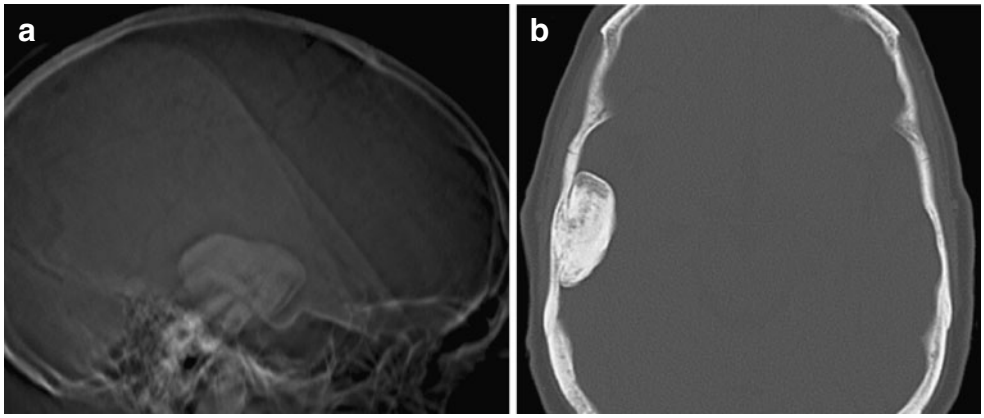

Fig. 8 Osteoma of the inner table in a 68-year-old woman. **a** Lateral skull radiograph revealing a well-defined dense lesion of the temporal bone. **b** CT scan with bone algorithm showing an ossified mushroom-like tumor with sharp borders attached by a bony stalk to the inner table

Osteomas appear as intensely homogeneous dense round (or oval) lesions on radiographs and CT, with the density being dependent upon the proportion of compact to cancellous bone. They emanate from one of the cortical tables and a bony stalk is usually observed (Fig. 8) [38]. They are homogeneously hypointense on T1WI and heterogeneously hypointense on T2WI and show no contrast enhancement. They do not disturb the diploë.

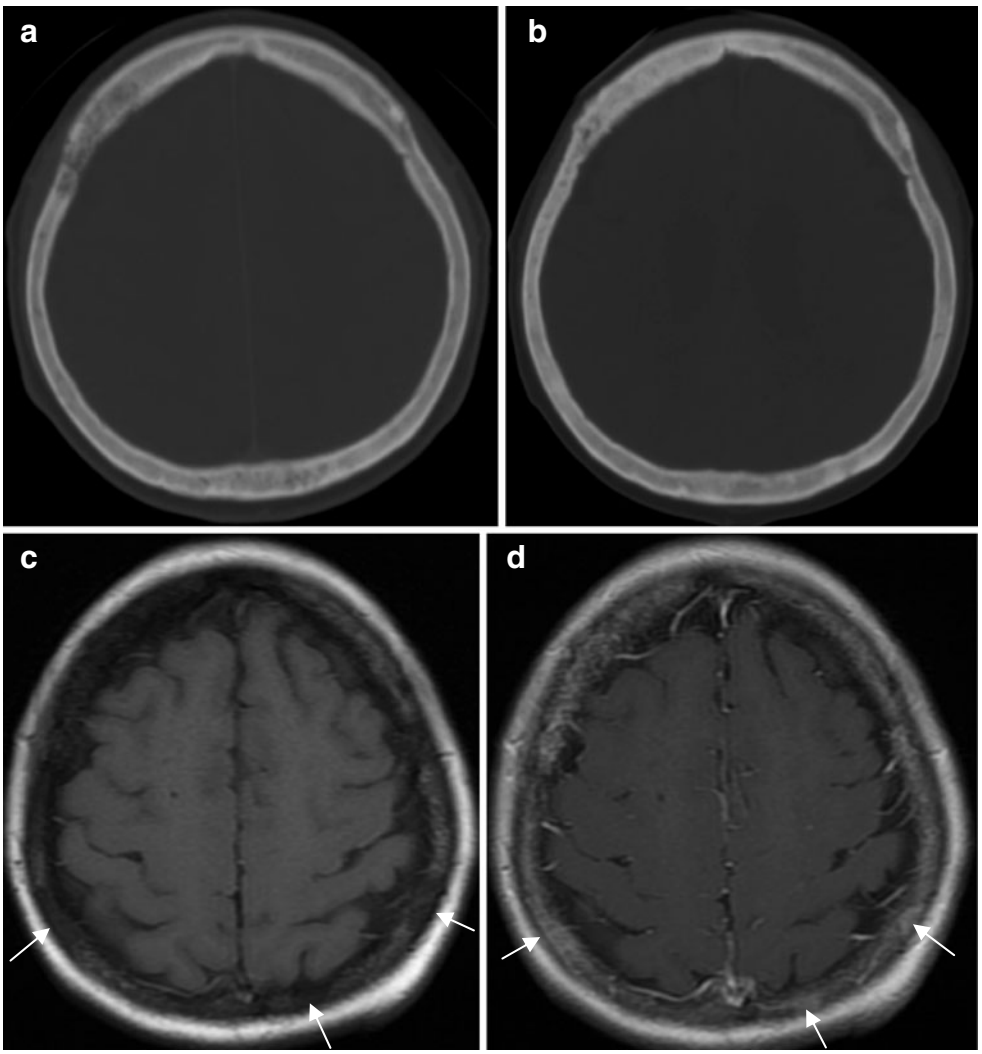

Fig. 9 Calvarial metastases in a 61-year-old woman diagnosed with small-cell lung carcinoma in 2005. **a** CT taken in 2006 showing a subtle permeative osteolytic lesion in the right frontal bone. **b** CT taken in 2007 showing an ill-defined osteoblastic lesion in the same area. The osteoblastic reaction may be due to treatment with antineoplastic agents. **c** In this T1WI (2007), the infiltrated right frontal bone is hypointense relative to the normal diploë of the left frontal bone. Also note the other areas of impaired signal throughout the calvaria *(arrows)*. **d** In this contrast-enhanced T1WI (2007), subtle, heterogeneous enhancement is observed at the sites of metastases. Note the more homogeneous appearance of the normal diploë of the left frontal bone

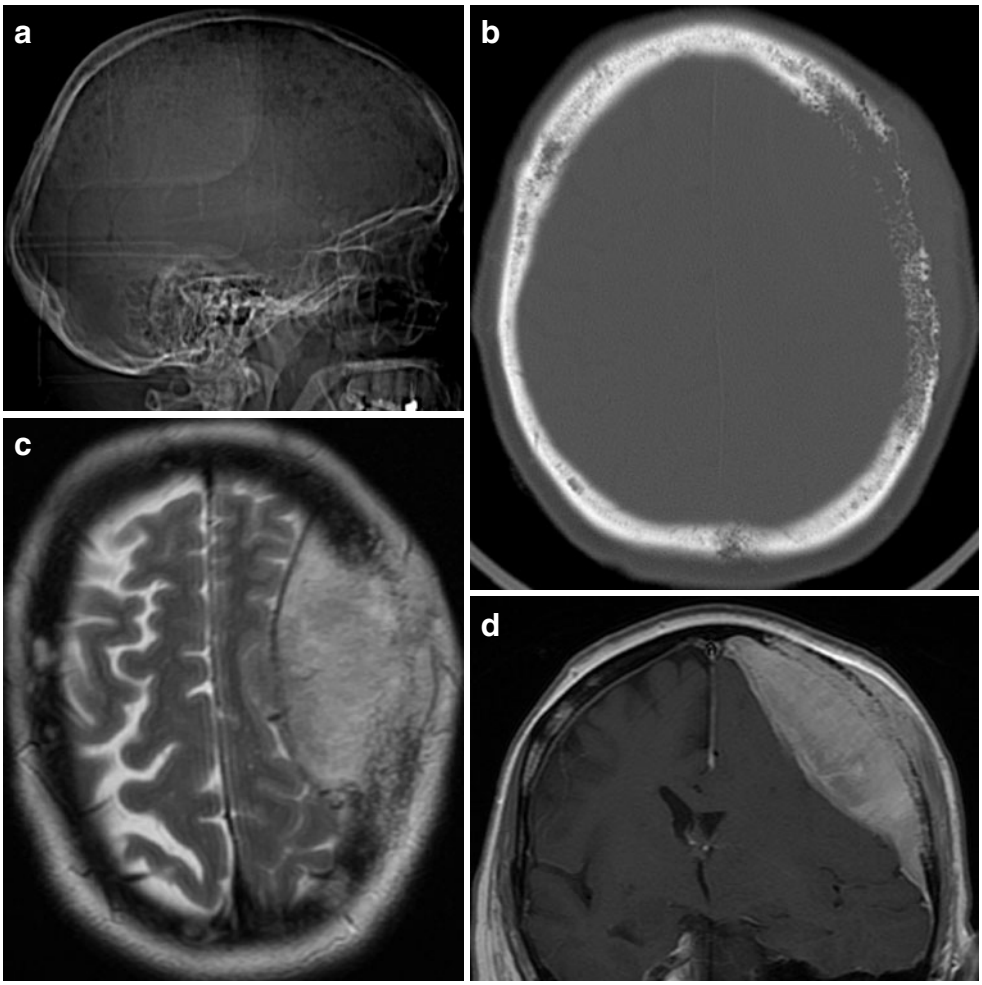

Fig. 10 Multiple myeloma in a 57-year-old-woman. **a** CT scout view taken in 2004 showing multiple, well-defined lytic lesions of roughly uniform size in the calvaria (myelomatosis). **b** CT with bone algorithm taken in 2007 showing progression of the disease with coalescence of lytic lesions in the left fronto-parietal region, extending both intra-and extracranially. Lytic lesions can be seen elsewhere in the calvaria. **c** Axial T2WI exhibiting a large lesion hyperintense to grey matter emanating from the diploë and other foci of hyperintesity in the diploë of the right calvaria. **d** Contrast-enhanced T1WI showing homogeneous enhancement of the lesions. Note the scattered foci of enhancement involving the right calvaria

Metastases

In contrast to those of the skull base, metastases to the skull vault are usually asymptomatic, but may still cause pain by irritating the pain-sensitive periosteum [39]. In adults, breast, lung, prostate, renal, and thyroid cancers and melanoma are the primary tumors that most commonly metastasize to the calvaria (in descending order) [40]. Calvarial metastases are

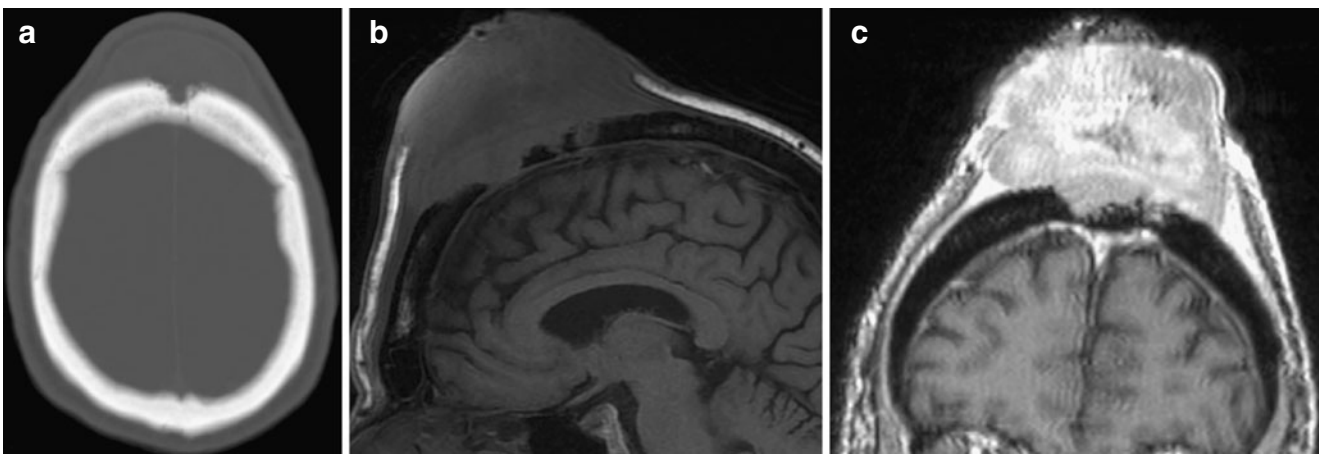

Fig. 11 Squamous cell carcinoma in a 60-year-old man. **a** CT in bone window showing a soft-tissue mass that is associated with bone destruction with an ill-defined border. **b** In an MRI taken 4 months later, T1WI shows that the lesion is isointense to grey matter and transverses the entire skull and even extends to the dura at several sites. **c** The lesion enhances heterogeneously following contrast administration

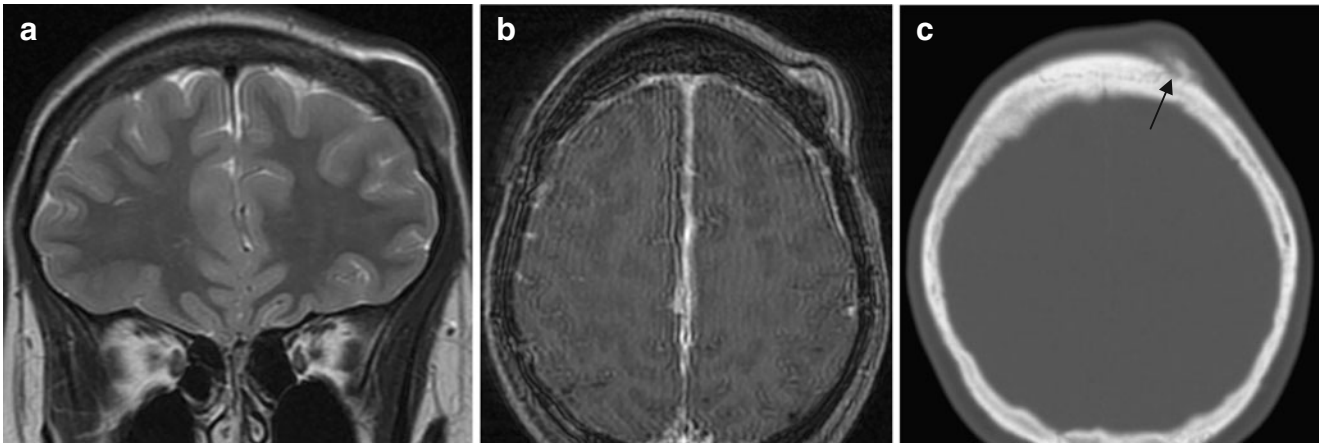

Fig. 12 Recurrent osteoblastic osteosarcoma in an 18-year-old woman with neurofibromatosis type II. **a** Coronal T2WI demonstrating a heterogeneous lesion that emanates from the outer table of the left frontal bone and infiltrates the superjacent soft tissue. **b** Axial contrast-enhanced T1WI showing avid enhancement of the entire lesion. **c** In this CT taken 15 months later, the lesion recurred rostral to the previous craniotomy. The ill-defined lesion shows lysis of the outer table *(arrow)* and variable mineralization of the superjacent soft tissue

usually diagnosed in the setting of a known malignancy. We encountered 14 cases of calvarial metastases, of which seven were the initial location of skeletal metastasis and three were the first evidence of an undiagnosed primary.

On radiographs and CT, metastatic deposits are most often osteolytic with ill-defined margins and an associated soft-tissue extension (Fig. 9). Metastases secondary to prostate cancer and osteosarcoma, in contrast, are predominantly osteoblastic, albeit with less hyperostosis than a meningioma [41]. Lung metastases demonstrate both a lytic and a blastic response, with the latter more prominent in response to effective chemotherapy [42]. Although calvarial metastases are sometimes solitary, there are usually multiple infiltrations. MRI, importantly, more clearly identifies small lesions, especially when contrast-enhanced. On T1WI, metastatic infiltrations appear hypointense to the background marrow in adults. Moreover, all areas of diploic enhancement (other than diploic veins and arachnoid granulations) can be interpreted as possible metastases. These areas of enhancement are most readily seen on fat-suppressed T1WI [5]. Osteolytic metastases appear as hyperintense to the background marrow on T2WI, whereas osteoblastic metastases appear as hypointense on both pulse sequences and may not enhance [4].

Multiple myeloma

Multiple myeloma (MM) is a malignant bone marrow neoplasm characterized by abnormal proliferation of monoclonal plasma cells. It usually disseminates throughout the axial skeleton, either multifocally or diffusely, and rarely does it present as a solitary lesion termed a plasmacytoma. The presenting symptom is usually bone pain [43].

Radiography is the primary diagnostic study for MM. Multifocal multiple myeloma, referred to as myelomatosis, results in a stippled pattern caused by multiple small, roundish osteolytic ("punched out") lesions with sharp, non-sclerotic margins of uniform size (Fig. 10). They may coalesce into larger segments of osteolysis. CT can

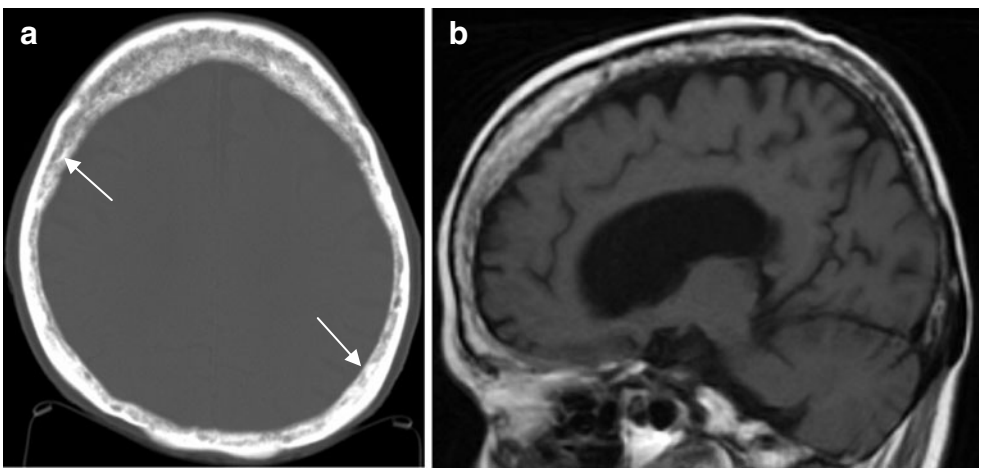

Fig. 13 Paget's disease (mixed phase) discovered incidentally in a 70-year-old woman. **a** CT showing thickening of both the outer table and of bony trabeculae within the calvaria (*arrows*). The thickening is less prominent in the frontal bone. **b** The diploë has increased signal intensity, especially in the frontal bone, in this sagittal T1WI

demonstrate a fuller extent of the disease and in some cases can show lesions not appreciated on radiography [44]. The signal intensities on MRI are similar to those of metastases; however, signal intensity abnormalities are not always present in myelomatous nodules [45]. MM may less commonly manifest in the calvaria as diffuse skeletal osteopenia where myeloma cells are intimately admixed with the hematopoietic cells without well-defined lytic lesions. This form is difficult to detect with CT and is best appreciated with MRI [46]. In contrast to metastases, which invariably involve secondary bone formation in response to the bone destruction, MM evolves as a purely lytic lesion [47]. As such, barring a skeletal complication such as bone fracture, it will not be detected with technetium 99-m based bone scans.

Squamous and basal cell carcinomas

Primary skin cancers of the scalp can secondarily invade the calvaria. These tumors predominate in men. A significant proportion of these tumors exhibit this tendency, partly because the subgaleal plane offers little resistance [48]. CT may show extremely ill defined osteolysis that begins at the outer table and can extend to the dura (Fig. 11) [49]. The solitary lesion shows the same intensities as metastasis on MRI. Occasionally, a calvarial metastasis that invades the skin secondarily can mimic a primary carcinoma of the scalp. All of the skin carcinomas in our series showed more extracranial involvement than intracranial involvement, a feature that can be helpful in distinguishing these tumors from metastasis.

Osteosarcoma

Osteosarcomas include a family of malignant neoplasms in which the malignant cells have the capacity to produce immature bone. These tumors rarely affect the skull vault and usually present in adolescents and young adults. When they arise in the calvaria later in life, they usually develop in the setting of pre-existing benign disease, such as Paget's disease or less commonly fibrous dysplasia, or previous radiation [50]. Only two calvarial osteosarcomas have presented at the MNI since 1970: one was osteoblastic and of primary origin (Fig. 12) and the other was secondary to Paget's disease.

As in the more commonly affected long bones, the osteosarcoma of the skull vault can be a lytic, blastic, or mixed-type [51]. Moreover, it usually presents with a wide zone of transition. CT helps identify the malignant nature of the lesion, shows the presence of new bone formation in the soft tissue component, and allows for accurate evaluation of intracranial extension [50]. MRI does not effectively show tumor calcification but can show soft-tissue involvement more clearly [52]. The lesion has low signal intensity on T1WI and a heterogeneous intensity on T2WI that depends on the matrix. For example, osteoblastic osteosarcoma has a relatively low signal appearance [53]. They enhance heterogeneously after contrast administration [21].

Paget's disease and Paget's sarcoma

Paget's disease, also known as osteitis deformans, is an incompletely understood, albeit most likely genetically based condition that entails abnormal and excessive bone remodeling [54]. It is typically discovered incidentally and affects 3% of the population over 40 years of age. When the skull is involved, as it is in about half the cases, the entire thickness of the bone is affected. The disease progresses through three phases: an osteolytic phase, followed by a mixed phase characterized by the development of cortical and trabecular coarsening and thickening, and finally followed by a blastic phase characterized by marked bone sclerosis and thickening of the skull (Fig. 13) [55]. During the osteolytic phase, a lucent rim often surrounds the lesion on CT [56]. The MRI appearance varies with the stage of the disease. On both T1 and T2WI, the mixed phase is heterogeneously hyperintense due to the repopulation of intratrabecular spaces by fat cells whereas the blastic phase is hypointense as bone replaces these fat cells [55].

Sarcomatous transformation of Paget's disease is a rare complication that has not presented at the MNI since the 1970s. The incidence of Pagetic sarcoma, which is most often an osteosarcoma, has declined to about 0.3% of patients [57]. It usually presents later in the course of the disease. Relative to most other Pagetic bones, the Pagetic skull rarely develops a sarcomatous neoplasm [58]. Interestingly, over half of the reported cases of benign giant-cell tumors associated with Paget's disease have been observed in patients whose ancestry traces to Campania, Italy. They preferentially involve the skull [59]. We have not encountered such a case.

Conclusions

Arriving at a definitive diagnosis for calvarial lesions based solely on imaging can be tricky. Nonetheless, radiographic, CT, and MRI imaging studies and evaluation of the adult patient's clinical history can help narrow the differential diagnosis.

Acknowledgements JG was supported by a McGill University Faculty of Medicine summer studentship.

Conflict of Interest The authors declare that they have no conflicts of interest.

References

1. Thomas J, Baker H. Assessment of roentgenographic lucencies of the skull: a systematic approach. Neurology. 1975;25:99–106.
2. Morón F, Morriss M, Jones J, Hunter J. Lumps and bumps on the head in children: use of CT and MR imaging in solving the clinical diagnostic dilemma. Radiographics. 2004;24:1655–74.
3. Amaral L, Chiurciu M, Almedia JR, Ferreira NF, Mendonça R, Lima SS. MR imaging for lesions of the cranial vault. Arq Neuropsiquiatr. 2003;61:521–32.
4. Bourekas EC, Lanzieri CF. The Calvarium. Semin Ultrasound CT MRI. 1994;15:424–53.
5. West MS, Russell EJ, Breit R, Sze G, Kim K. Calvarial and skull based metastases: comparison of nonenhanced and Gd-DPTA-enhanced MR images. Radiology. 1990;174:85–91.
6. Curnes JT. MR imaging of peripheral intracranial neoplasms: extraaxial versus intraaxial masses. J Comp Ass Tomogr. 1987;11: 932–7.
7. George AE, Russell EJ, Kricheff I. White matter buckling: CT sign of extra-axial intracranial mass. AJR. 1980;135:1031–6.
8. Greenspan A, Jundt G, Remagen W. Radiologic and pathologic approach to bone tumors. In: Differential diagnosis in orthopaedic oncology. 2nd ed. Philadelphia, PA: LWW, 2007; 1–39.
9. Arana E, Marti-Bonmati L, Ricart V, Pérez-Ebrí M. Dural enhancement with primary calvarial lesions. Neuroradiology. 2004;46:900–5.
10. Eisen M, Yousem D, Montone K, et al. Use of preoperative MR to predict dural, perineural, and venous sinus invasion of skull base tumors. AJNR. 1996;17:1937–45.
11. Meltzer C, Fukui M, Kanal E, Smirniotopoulos J. MR imaging of the meninges. Part 1. Normal anatomic features and nonneoplastic disease. Radiology. 1996;201:297–308.
12. Ahmadi J, Hinton DR, Segall HD, Couldwell WT, Stanley RB. Dural invasion by craniofacial and calvarial neoplasms: MR imaging and histopathologic evaluation. Radiology. 1993;188:747–9.
13. Stull MA, Kransdorf MJ, Devaney KO. From the archives of the AFIP: Langerhans cell histiocytosis of bone. Radiographics. 1992;12:801–23.
14. Beltran J, Aparisi F, Bonmati LM, Rosenberg ZS, Present D, Steiner GC. Eosinophilic granuloma: MRI manifestations. Skeletal Radiol. 1993;22:157–61.
15. Okamoto K, Ito J, Furusawa T, Sakai K, Tokiguchi S. Imaging of eosinophilic granuloma. Neuroradiology. 1999;41:723–8.
16. De Schepper AMA, Ramon F, Van Marck E. MR imaging of eosinophilic granuloma: report of 11 cases. Skeletal Radiol. 1993;22:163–6.
17. Ortiz O, Schochet S. Bastug D. Imaging evaluation and clinicopathologic correlation of mass lesions involving the calvaria Part II: tumoral and inflammatory lesions Int J Neuroradiol. 1999;5:151–65.
18. Smirniotopoulos JG, Chiechi MV. From the archives of the AFIP: teratomas, dermoids, and epidermoids of the head and neck. Radiographics. 1995;15:1437–55.
19. Arana E, Latorre FF, Revert A, et al. Intradiploic epidermoid cysts. Neuroradiology. 1996;38:306–11.
20. Gormley WB, Tomecek FJ, Qureshi N, Malik GM. Craniocerebral epidermoid and dermoid tumours: a review of 32 cases. Acta Neurochir (Wien). 1994;128:115–21.
21. Chung E, Murphey MD, Specht CS, Cube R, Smirniotopoulos JG. From the archives of the AFIP: pediatric orbital tumors and tumorlike lesions: osseous lesions of the orbit. Radiographics. 2008;28:1193–214.
22. Khanam H, Lipper M, Wolff CL, Lopes MBS. Calvarial hemangiomas: report of two cases and review of the literature. Surg Neurol. 2001;55:63–7.
23. Heckl S, Aschoff A, Kunze S. Cavernomas of the skull: review of the literature 1975–2000. Neurosurg Rev. 2002;25:56–62.
24. Peterson DL, Murk SE, Story JL. Multifocal cavernous hemangioma of the skull: report of a case and review of the literature. Neurosurgery. 1992;30:778–82.
25. Politi M, Romeike BFM, Papanagiotou P, Nabhan A, Struffert T, Feiden W, et al. Intraosseous hemangioma of the skull with dural tail sign: radiologic features with pathologic correlation. AJNR. 2005;26:2049–52.
26. Buetow MP, Buetow PC, Smirniotopoulos JG. From the archives of the AFIP: typical, atypical, and misleading features in meningioma. Radiographics. 1991;11:1087–106.
27. Ginsberg L. Radiology of meningiomas. J Neurooncol. 1996;29: 229–38.
28. Daffner RH, Yakulis R, Maroon JC. Intraosseous meningioma. Skeletal Radiol. 1998;27:108–11.
29. Rausching W. Meningiomas and other non-glial neoplasms. In: Osborn AG, editor. Diagnostic neuroradiology. 1st ed. St. Louis, MO: Mosby; 1994. pp. 579–625.
30. Arana E, Diaz C, Latorre FF, Menor F, Revert A, Beltrán A, et al. Primary intraosseous meningiomas. Acta Radiol. 1996;37:379– 42.
31. Ruscalleda J, Feliciani M, Avila A, Castanier E, Guardia E, de Juan M. Neuroradiological features of intracranial and intraorbital meningeal haemangiopericytomas. Neuroradiology. 1994;36:440–5.
32. Guthrie BL, Ebersold MJ, Scheithauer BW, Shaw EG. Meningeal hemangiopericytoma: histopathological features, treatment, and long-term follow-up of 44 cases. Neurosurgery. 1989;25:514– 22.
33. Lafond-Kim GM, Diler DG, Hou J, Riben MW, Jennings TA. Osseous hemangiopericytomas of unsuspected intracranial origin. Skeletal Radiol. 1998;27:98–102.
34. Sibrain NA, Butt S, Connor SEJ. Imaging features of central nervous system haemangiopericytomas. Eur Radiol. 2007;17: 1685–93.
35. Obisesan AA, Lagundoye SB, Daramola JO, Ajagbe HA, Oluwasanmi JO. The radiological features of fibrous dysplasia of the craniofacial bones. Oral Surg Oral Med Oral Pathol. 1977;44:949–59.
36. Shah ZK, Peh WCG, Loh WL, Shek TWH. Magnetic resonance imaging appearances of fibrous dysplasia. Br J Radiol. 2005;78: 1104–15.
37. Jee WH, Choi KH, Choe BY, Park JM, Shinn KS. Fibrous dysplasia: MR imaging characteristics with radiopathologic correlation. AJR. 1996;167:1523–7.
38. Avrahami E, Even I. Osteoma of the inner table of the skull-CT diagnosis. Clinical Radiology. 2000;55:435–8.
39. Posner, PB. Metastases. In: Neurologic complications of cancer. 1st ed. Philadelphia, PA: F.A. Davis Company, 1995:108–109.
40. Newton HB. Skull and dural metastases. In: Schiff D, Kesari S, Wen PY, editors. Cancer: neurology in clinical practice. 2nd ed. Totowa, NJ: Humana Press; 2008. pp. 145–61.
41. Arana E, Martí-Bonmatí L. CT and MRI of focal calvarial lesions. AJR. 1999;172:1683–8.
42. Stattaus J, Hahn S, Gauler T, Eberhardt W, Mueller SP, Forsting M, et al. Osteoblastic response as a healing reaction to chemotherapy mimicking progressive disease in patients with small cell lung cancer. Eur Radiol. 2009;19:193–200.
43. Angtuaco EJC, Fassas ABT, Walker R, Sethi R, Barlogie B. Multiple myeloma: clinical review and diagnostic imaging. Radiology. 2004;231:11–23.
44. Schreiman JS, McLeod RA, Kyle RA, Beabout JW. Multiple myeloma: evaluation by CT. Radiology. 1975;154:483–6.
45. Libshitz HI, Malthouse SR, Cunningham D, MacVicar AD, Husband JE. Multiple myeloma: appearance at MR imaging. Radiology. 1992;182:833–7.

46. Delorme S, Baur-Melnyk A. Imaging in multiple myeloma. Eur J Radiol. 2009;70:401–8.
47. Roodman GD. Mechanisms of bone metastasis. N Engl J Med. 2004;350:1655–64.
48. Lang PG, Braun MA, Kwatra R. Aggressive squamous cell carcinomas of the scalp. Dermatological Surgery. 2006;32:1163–70.
49. Sakamoto T, Mineura K, Kikichi K, Kowada M. Intracranial invasion of scalp carcinoma: report of five cases. Acta Neurochir (Wien). 1989;98:66–9.
50. Haque F, Fazal ST, Ahmad SA, Abbas SZ, Naseem S. Primary osteosarcoma of the skull. Australian radiology. 2006;50:63–5.
51. Kornreich L, Grunebaum M, Ziv N, Cohen Y. Osteogenic sarcoma of the calvarium in children: CT manifestations. Neuroradiology. 1988;30:439–41.
52. Shramkek JK, Kassner EG, White SS. MR appearance of osteogenic sarcoma of the calvaria. AJR. 1992;158:661–2.
53. Sundaram M, McGuire MH, Herbold DR. Magnetic resonance imaging of osteosarcoma. Skeletal Radiol. 1987;16:23–9.
54. Ralston SH, Langston AL, Reid IR. Pathogenesis and management of Paget's disease of bone. Lancet. 2008;372:155–63.
55. Smith SE, Murphey MD, Motamedi K, Mulligan ME, Resnik CS, Gannon FH. From the archives of the AFIP: radiologic spectrum of Paget disease of bone and its complications with pathologic correlation. Radiographics. 2002;22:1191–216.
56. Brouard R, Wybier M, Miquel A, Laredo JD. The lucent rim: a radiographic and computed tomography sign of Paget's disease of the skull. Eur Radiol. 2006;16:1306–11.
57. Mangham DC, Davie MW, Grimer RJ. Sarcoma arising in Paget's bone: declining incidence and increasing age at presentation. Bone. 2009;44:431–6.
58. Wick MR, Siegal GP, Unni KK, McLeod RA, Greditzer HG. Sarcomas of bone complicating osteitis deforroans (Paget's disease). Am J Surg Pathol. 1981;5:47–59.
59. Rendina D, Gennari L, De Filippo G, et al. Evidence for increased clinical severity of familial and sporadic Paget's disease of bone in Campania, southern Italy. J Bone Miner Res. 2006;21:1828–35.